

A Model for Third Sound Attenuation in Thick ^4He Films

K. Penanen and R. E. Packard

University of California at Berkeley, Physics Department, Berkeley, California 94720
E-mail: penanen@socrates.berkeley.edu

(Received February 20, 2002; revised March 15, 2002)

Third sound attenuation in thick ^4He films has been observed to be much greater than predictions based on known mechanisms. We propose a possible mechanism for this observed high attenuation. Pinned vortices, possibly created when the superfluid transition is traversed, undergo driven oscillations in the third sound wave flow field. The dissipation is caused by two related effects. The first is due to the mutual friction between the vortex cores and the normal component. The second, larger contribution, is due to the drag experienced by a vortex-induced surface dimple. Variations in vortex density explain quite naturally the observed lack of reproducibility in attenuation measurements. A vortex density on the order of 10^{17} m^{-2} is required to account for dissipation reported in several experiments. We discuss the temperature, frequency and thickness dependence of the dissipation. The proposed model is also applicable to a vortex contribution to fourth sound attenuation. If third sound attenuation is indeed a signature of a very dense array of pinned vorticity, then our conception of a homogeneous superfluid film needs considerable alteration.

Third sound is a surface thickness wave in superfluid helium films analogous to a shallow water gravity wave, with the Van der Waals interaction playing the role of gravity. These long-wavelength excitations have been observed in both ^4He (Refs. 1 and 2) and ^3He (Ref. 3), and have been a subject of extensive studies over the years. Among the phenomena well understood in the context of the existing theory⁴⁻⁶ are the temperature and thickness dependence of the third sound velocity and the suppression of the superfluid transition in thin films.⁷ However, a significant disparity persists between theory and experiment for third sound attenuation in thick films. The original third sound attenuation mechanism, implicitly suggested by

Atkins,⁴ was that of dissipative evaporation/re-condensation at the film surface. Due to effective viscous clamping of the normal component, the thickness variations in a wave result in temperature variations, with warmer regions corresponding to wave troughs. The film evaporates at a higher rate in thinner regions and condenses in thicker, colder regions. The result of this process is an attenuation of the wave amplitude and a correction to the propagation velocity. This model was further modified by Bergman^{5,6} to include the effects of heat transfer between the film and the substrate and to take into account temperature variation in the vapor. Finally, the effect of finite geometries was considered by van Beelen and Bannink⁸ (long capillary and parallel plates) and Brouwer *et al.*⁹ (parallel plate geometry). Although the modifications to the original model improved the agreement with experiment for thin unsaturated films (< 20 atomic layers, $1 \text{ a.l.} = 3.6 \text{ \AA}$), they all exhibit the same disparity with thick film experiments.

Published experimental data on third sound attenuation in thick films is remarkably scarce.^{1,2,10,11} The measured values vary widely with substrate material and surface preparation and even from run to run on the same substrate.² The typical observed attenuation is 50 to 1000 times larger than predicted by the evaporation/condensation model. Any experimentally measured attenuation includes not only "intrinsic" attenuation but also experimental artifacts such as incomplete reflection from the boundaries, diffractive losses, etc. Therefore, published attenuation figures are necessarily only an upper bound. However, the observed discrepancies appear to be too significant to be explained by these artifacts alone.

In the model we are proposing, vortices pinned at protrusions of the substrate are driven by the Magnus force generated by the third sound velocity oscillations. The dissipation is then a result of two related effects. One is the mutual friction between the vortex cores and the normal component of the fluid in the two fluid model. The other contribution is due to the drag force experienced by a vortex-induced surface dimple.¹²

Ellis and Luo¹³ have previously suggested that a two-dimensional analog of mutual friction or drag could be responsible for third sound decay in thin films at low temperatures. The presence of a high *net* density, in excess of 10^9 m^{-2} vortices in superfluid helium films was conjectured by Ellis *et al.*^{14,15} from the measured Doppler splitting of degenerate modes in an annular third sound resonator. The *total* density, i.e., sum of clockwise and counterclockwise vortex densities, can be significantly higher but could not be independently measured. Vortices may remain in the film after the film undergoes the Kosterlitz–Thouless⁷ transition. The transition can be crossed either while cooling an already present thick film, or while the film thickness is increased if the film is formed at a low temperature. Due to the high binding energy (100 K for a 1 nm protrusion), the vortices can remain

trapped indefinitely at the imperfections on the substrate surface. Thus a thick superfluid film may be a very “dirty” superfluid, filled with a high density of trapped vortices.

Due to a number of simplifying assumptions, the calculations we present are meant to provide only a semi-quantative description of the attenuation. We assume the temperature to be much lower than the bulk superfluid temperature T_c , so that the superfluid mass density ρ_s is approximately equal to the total density ρ . For a comparison to Bergman’s results^{5,6} we use the same Van der Waals substrate potential.^{16,17} We assume that flow velocity and deflection amplitudes are small.

We first consider the attenuation due to the mutual friction between the vortex cores and the normal component, ignoring surface effects. This case is directly applicable to the attenuation of fourth sound in a parallel plate geometry and forms a foundation for calculations which include the effects of free surface.

In the presence of flowing superfluid, a pinned vortex is deflected from its equilibrium position by the Magnus force (per unit length) $F_M = \rho_s v \kappa$, where κ is the quantum of circulation $\kappa = h/m_4$ and v is the flow velocity. While moving through the normal component, which is considered to be at rest, the vortex core experiences a dissipative drag force (per unit length) (for a review, see Ref. 18, and references therein), given by:

$$f_D = \gamma_0 v_{\text{core}}. \quad (1)$$

In the low temperature regime $\gamma_0 = \frac{B\kappa\rho_n}{2}$ where B is a dimensionless parameter of order 1, weakly dependent on temperature and frequency. The dynamics of the vortex motion needs to be considered to estimate the magnitude of the dissipation due to mutual friction. The shape of the vortex is determined by its tension N , bending energy and boundary conditions. Boundary conditions require that the vortex line be normal both to the substrate and the free surface.

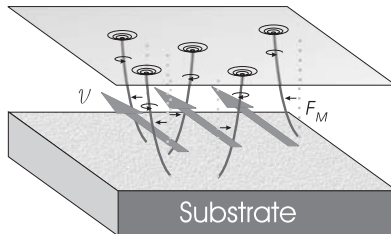


Fig. 1. Trapped vortices are deflected by Magnus force F_M due to velocity field v generated in the third sound wave.

The tension N , or energy per unit length, is

$$N = \frac{\rho_s \kappa^2}{4\pi} \ln \frac{R}{a_0} \quad (2)$$

In the choice of a_0 the intrinsic energy of the core is included. The size R is the characteristic length scale in the system and is taken here to be the average spacing between the vortices. A contribution due to bending energy becomes significant when the curvature radius becomes smaller than R . The effects of the hard wall and the curvature manifest themselves in films thinner than $\approx 10 \text{ \AA}$, and can be ignored for thicker films.

If bending energy is ignored, for small displacement the tension is the same along the vortex line and the curvature, $\frac{d^2 \Delta x}{dz^2} = F_M/N$, is constant. Since at the free surface the vortex is normal to the surface, the displacement from the equilibrium position as a function of the distance from the substrate is:

$$\Delta x(z, t) = \frac{z(2d-z) F_M(t)}{2N}, \quad (3)$$

where d is the film thickness. A graph of Δx vs. z in a thick film is shown in Fig. 2. For a third sound wave generating oscillating local film velocity with amplitude v_0 and having angular frequency ω , the vortex core velocity is:

$$v_{\text{core}}(z, t) = i\omega \Delta x(z, t) = \frac{i\omega z(2d-z) v_0 e^{i\omega t} \kappa \rho_s}{2N}. \quad (4)$$

The energy dissipated in the film due to a single vortex per oscillation period is the product of the vortex core velocity and the drag force, integrated over the z coordinate up to the film thickness d , integrated over the oscillation period

$$\Delta E = \int_0^{\frac{2\pi}{\omega}} \int_0^d \gamma_0 v_{\text{core}}^2(z, t) dz dt \quad (5)$$

$$\Delta E = \frac{2\pi\omega v_0^2 \gamma_0 d^5 \kappa^2 \rho_s}{15N^2} \quad (6)$$

The amount of energy stored in the third sound wave (per unit area) is

$$E = \frac{\rho v_0^2 d}{2} \quad (7)$$

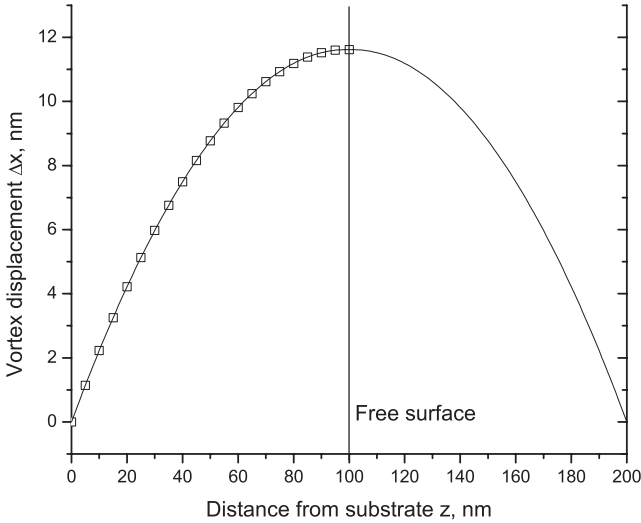


Fig. 2. Equilibrium vortex displacement Δx as a function of distance from the substrate z in a 10 cm/s flow field for a thick (100 nm) film (hollow squares). Also shown is the vortex displacement in the fourth sound velocity field in a parallel plate geometry with plate separation of 200 nm (solid line), assuming the pinning sites on the opposite sides lie directly across.

If the density of the vortices per unit area is $n = \frac{1}{\pi R^2}$, the inverse of the quality factor, Q^{-1} of a third sound resonator can then be calculated to be

$$Q^{-1} = \frac{\Delta E}{2\pi E} = \frac{128\pi^2}{15} n \frac{\gamma_0}{\rho} d^4 \frac{\omega}{\kappa^2} \left(\ln \frac{1}{\pi n a_0^2} \right)^{-2} \quad (8)$$

A more commonly cited measured quantity is the third sound attenuation α

$$\alpha_{\text{core}} = \frac{\omega}{2Qc_3} = \frac{64\pi^2}{15} n \frac{\gamma_0}{\rho} d^4 \frac{\omega^2}{c_3 \kappa^2} \left(\ln \frac{1}{\pi n a_0^2} \right)^{-2} \quad (9)$$

where c_3 is the speed of third sound. The temperature dependence of the quality factor (and the attenuation coefficient) in the low temperature regime are dominated by the normal component density ρ_n in γ_0 : $\alpha_{\text{core}} \propto \rho_n / \rho$. The temperature dependence of α_{core} for a 36 nm film at 1000 Hz is displayed in Fig. 3. At a given temperature, the thickness dependence is $Q \propto d^{-4}$. For the attenuation α_{core} there is an additional thickness dependence because the third sound velocity, c_3 , also depends on thickness. The power law for this dependence is determined by the exponent in the

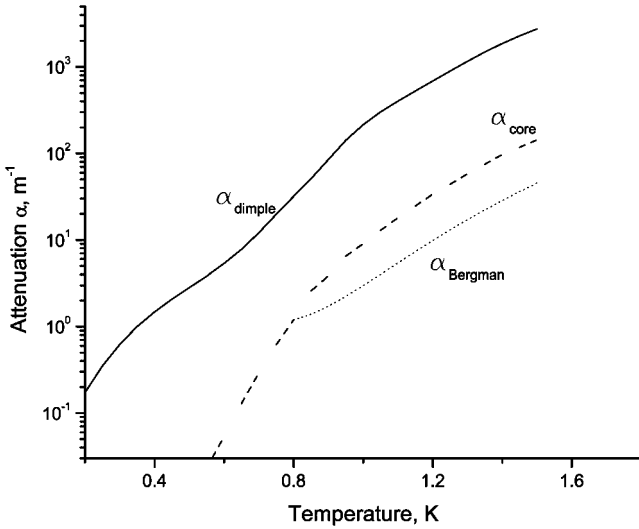


Fig. 3. Calculated attenuation α as a function of temperature for the Atkins–Bergman theory in the thick film regime (dotted line), proposed model without contribution from vortex dimples (dashed line) and the proposed model with vortex dimple contribution (solid line). Film thickness is 100 layers (360 Å) for all three cases; vortex density $n = 5 \times 10^{17} \text{ m}^{-2}$ is used in the two vortex drag models. Frequency is 1000 Hz. The Atkins–Bergman theory is expected to break down below ≈ 0.8 K, when the mean free path exceeds the typical cell dimensions.

Van der Waals force. For thinner films $c_3 \propto d^{-3/2}$ and for thicker films $c_3 \propto d^{-2}$, giving a $d^{11/2}$ to d^6 dependence for the attenuation. Equation (8), with no modifications, also describes attenuation of fourth sound if helium is confined between parallel plates separated by $2d$.

For comparison, we also calculate the temperature, thickness and frequency dependence for the Atkins/Bergman theory.^{5,6} In the thick film regime, where evaporation/re-condensation mechanism dominates over heat conduction through substrate and vapor, the complex third sound velocity can be determined using a simplified expression (see Eq. (30) in Ref. 6):

$$\frac{g_{\text{eff}} d \rho_s}{c_3^2 \rho} \left(1 + \frac{TS}{L} \right)^2 = \left[1 - \frac{9}{32} \frac{k_B T}{m} \frac{i \omega \rho}{A g_{\text{eff}}} \left(\frac{TS}{L} \right)^2 \left(1 - \frac{\rho_g}{\rho} \left(1 + \frac{TS}{L} \right)^{-2} \right) \right]^{-1}, \quad (10)$$

where $A \equiv \frac{1}{2} \rho_g (k_B T / 2\pi m_4)^{1/2}$. In this equation, g_{eff} is the effective Van der Waals acceleration (force per unit mass) at the free surface, ρ_s is the

average superfluid density in the film, ρ is the film density, T , S and L are the film temperature, specific entropy and latent heat and ρ_g is the saturated vapor density at temperature T . In this equation the third sound velocity c_3 is a complex number, in which the imaginary component describes the attenuation: $\alpha = 2\omega \text{Im}(1/c_3)$. At low temperatures, where the imaginary part of Eq. (10) is small, α can be approximated as:

$$\alpha_{\text{Bergman}} = \frac{9}{64} \sqrt{\frac{1}{g_{\text{eff}} d}} \frac{k_B T}{m} \frac{\omega^2 \rho}{A g_{\text{eff}}} \left(\frac{TS}{L}\right)^2. \quad (11)$$

The attenuation α scales as $d/(g_{\text{eff}} d)^{3/2}$, or $d^{11/2}$ to d^6 , depending on the Van der Waals potential exponent. The temperature dependence enters through T , S , L and ρ_g . In the temperature range where the mean free path in the vapor is shorter than the typical system size, where the Atkins/Bergman theory theory is applicable ($T > 0.8$ K), the temperature dependence is similar to that in the vortex drag model, as shown in Fig. 3. Both theories predict frequency dependence $\alpha \propto \omega^2$.

For a given density of trapped vortices, a more significant contribution to the attenuation will come from the drag experienced by the the vortex dimples at the free surface.¹² High flow velocities near the vortex core lead to an additional kinetic term in the chemical potential, causing the formation of a surface depression, or dimple. The dimple size and shape are determined by the equilibrium between the Bernoulli thinning, Van der Waals potential of the substrate and the surface tension. Although the lateral size of these dimples is large, on the order of 10^{-6} m for the bulk free surface, in a typical saturated film several tens of nanometers thick it is localized to several nanometers.

We will consider quasi-static vortex motion, in which the vortex profile is at all times determined by the local third sound velocity field. This would be the case as long as the effective mass of the vortex dimple is small enough, or the third sound frequency is low enough:

$$\omega^2 \ll \frac{N}{m_{\text{eff}} d}, \quad (12)$$

where m_{eff} is the effective mass of the dimple. Under these conditions the displacement of the dimple can be evaluated using the solution for the displacement of free end of the vortex from Eq. (3) with $z = d$.

$$\Delta x(t) = \frac{d^2 F_M(t)}{2N}. \quad (13)$$

The effective mass of the dimple is of the order of the mass of displaced liquid. We use Eq. (19) from Ref. 12 describing the dimple profile to evaluate the volume (and the effective mass) of the dimple. Inverting and numerically integrating that equation gives a displaced mass of $9.8 \times 10^6 m_4$ for a 100 layer (360 Å) thick film, suggesting that condition (12) is satisfied for all realistic experimental situations.

A detailed numerical solution for the drag force experienced by the vortex dimple is beyond the scope of this paper. However, to make an order of magnitude estimate we note that the typical cross-sectional area of the dimple is similar to that of a bubble created around a negative ion. We can use the available data on the mobility of negative ions in helium.¹⁹ At low temperatures, this problem is treated as scattering of quasi-particles in the ballistic regime, enhanced by resonant S-wave phonon scattering due to the bubble “breathing” mode.²⁰ The effect of the resonant enhancement is 1 to 2 orders of magnitude increase in scattering cross section compared to the geometrical estimate. At temperatures above ≈ 0.55 K, where the roton contribution becomes dominant and the resonant scattering effects do not dominate, the mobility scales inversely with the geometric cross section.²⁰ We can estimate the drag on the dimple as

$$F_{\text{drag}} = -\frac{|e|}{\mu_-(T)} \frac{\sigma_{\text{dimple}}}{\sigma_-} v, \quad (14)$$

where e is the electron charge, μ_- is the (measured) negative ion mobility, σ_{dimple} is the calculated geometric cross section of the vortex dimple and σ_- is the generally accepted geometric cross section of the negative ion bubble, πr^2 , $r \approx 15.4$ Å.²¹

The attenuation factor calculated using the dimple model is larger than that due to vortex core alone:

$$\alpha_{\text{dimple}} = \alpha_{\text{core}} \frac{|e|}{\mu_-(T)} \frac{\sigma_{\text{dimple}}}{\sigma_-} \frac{15}{4B\rho_n d\kappa} \quad (15)$$

The results of this calculation are plotted in Fig. 3. This estimate will become invalid when the mean free path of the excitations becomes smaller than the dimple size, typically above 1.5 K, at which point a viscous drag description becomes applicable. The estimate is also expected to require significant dimple-size-dependent corrections at low temperatures, $T < 0.6$ K, where resonant phonon scattering is significant. The parameters of a particular system should be considered for making quantitative predictions.

The frequency dependence of the vortex dimple attenuation model is the same as in both the Bergman-Atkins and the vortex core models, i.e.,

$\alpha \propto \omega^2$. The film thickness dependence enters through both dimple size and dimple displacement. In the regime where attenuation is proportional to the geometric cross section, numerical integration shows for the thickness range 10 to 1000 nm this dependence can be approximated as $\alpha \propto d^{6.75}$. This compares to $\alpha \propto d^{5.5}$ for the Atkins–Bergman and the vortex core models.

Assuming that the attenuation is dominated by the drag experienced by the vortex dimple, one can estimate the density of trapped vortices in helium films which would account for the observed attenuation. Table I summarizes attenuation data from Everitt *et al.*² and Telschow *et al.*¹¹ We calculate the discrepancy between the measured values for attenuation and the values predicted by the Atkins/Bergman theory. We also calculate the density of vortices required to account for the observed attenuation if the vortex dimple drag model is applied.

The implications of the model described above is that the purely thermodynamic treatment of helium films may not be adequate when considering third sound attenuation and related phenomena. The model naturally accounts for the observed lack of reproducibility of attenuation measurements. However, vortex densities required to account for the observed attenuation using the proposed model are very high, in excess of 10^{17} m^{-2} . In the presence of high density of vortices one could hypothesize other mechanisms producing additional attenuation, such as vortex creep, dimple-dimple interaction, production of ripplons, etc. If any of these or other vortex-related mechanisms produce significant additional attenuation, lower densities would be sufficient. In the framework of the presented

Table I

Attenuation of Third Sound α , Measured at Different Thicknesses d , Temperatures T and Frequencies f . The Two Entries for Everitt *et al.*² Refer to Two Data Sets Taken on Different Days on the Same Substrate. Telschow *et al.* Point Out that Their Measurement Provides an *Upper Bound* of Attenuation. Film Thicknesses Were Not Independently Measured by Telschow *et al.*, and Were Calculated Here from Ellipsometry Measurements on Stainless Steel (Everitt *et al.*²) and x-Ray Reflectivity Measurements on Silicon (Lurio *et al.*²³). To Minimize the Effect of Uncertainty in Film Thickness d , Experimental Values for the Third Sound Velocity $c_3^2 \propto g_{\text{eff}} d$ Are Used Where Possible. The Vortex Densities, n , Are Calculated Using the Dimple Model. These Values Are an Upper Limit if Additional Vortex Effects Increase the Third Sound Attenuation

Source	Substrate	d (Å)	T (K)	f (Hz)	c_3 (m/s)	α (m ⁻¹)	$\frac{\alpha}{\alpha_{\text{Bergman}}}$	n (m ⁻²)
Everitt <i>et al.</i> ²	polished stainless steel	245	1.2	1000	1.6	175	270	9×10^{17}
Everitt <i>et al.</i> ²	polished stainless steel	245	1.2	1000	1.6	220	340	1.1×10^{18}
Telschow <i>et al.</i> ¹¹	untreated stainless steel	300	1.3	0.8	1.2	0.05	8600	6×10^{18}
Telschow <i>et al.</i> ¹¹	glass	220	1.3	40	0.92	1.7	170	1.2×10^{18}
Telschow <i>et al.</i> ¹¹	glass	180	1.3	200	1.24	3	42	6×10^{17}

model, a more rigorous calculation may likewise produce higher attenuation, implying lower densities to account for the measured attenuation.

The swirling experiments of Ellis *et al.*^{14,15} demonstrated a net vortex density on the order of 10^9 m^{-2} , but were not sensitive to the total (sum of clockwise and counterclockwise) density. The densities shown in Table I are also higher than the values estimated to explain the contact angle in film spreading measurements of Luusalo *et al.*²² Two points concerning those results can be made. First, in the calculation for the limiting vortex density only the flow field of a single nearby vortex was used. The actual limiting vortex density can be higher, since the flow field of several neighboring vortices may partially cancel. Also, in the energy minimization in the calculation for the film thickness the pressure from the vortex tension was assumed to be uniform. The presence of vortex dimples will modify the equilibrium condition so that for the same thinning a larger density of vortices will be required.

To check the validity of the proposed model, more experimental work needs to be done. The trapped vortex density may be sensitive to the cooling rate at which the superfluid transition is traversed. The vortex density may also be reduced by forming the film starting from a very thick bulk puddle by lowering the liquid level in the cell. Following Ellis *et al.*^{14,15} one could also attempt to de-pin the vortices by driving a high amplitude third sound wave or DC current. The effect of such large density of vortices and associated surface deformation might also be detectable in optical or x-ray scattering experiments.

Thick superfluid ^4He films have usually been perceived as homogeneous and isotropic. A large variety of experiments have been interpreted in terms of this conceptual framework. Based on the anomalously high third sound attenuation in thick films, it seems possible that these films are packed with a very dense array of random vortices with spacing approaching a few tens of nanometers. It will be interesting to see if this conceptual shift stands the scrutiny of experiment.

ACKNOWLEDGMENTS

We acknowledge helpful discussion with G. A. Williams. This work was supported by the National Science Foundation and NASA.

REFERENCES

1. C. W. F. Everitt, K. R. Atkins, and A. Denenstein, Detection of third sound in liquid helium films, *Phys. Rev. Lett.* **8**, 161 (1962).
2. C. W. F. Everitt, K. R. Atkins, and A. Denenstein, Third sound in liquid helium films, *Phys. Rev. A* **136**, 1494 (1964).

3. A. M. R. Schecter, R. W. Simmonds, R. E. Packard, and J. C. Davis, Observation of "third sound" in superfluid He-3, *Nature* **396**, 554 (1998).
4. K. R. Atkins, Third and fourth sound in liquid helium II, *Phys. Rev.* **113**, 962 (1959).
5. D. Bergman, Hydrodynamics and third sound in thin He II films, *Phys. Rev.* **188**, 370 (1969).
6. D. J. Bergman, Third sound in superfluid helium films of arbitrary thickness, *Phys. Rev. A* **3**, 2058 (1971).
7. J. M. Kosterlitz and D. J. Thouless, Ordering, metastability and phase transition in two-dimensional systems, *J. Phys. C* **6**, 1181 (1973).
8. H. van Beelen and G. Bannink, The propagation of 3rd-sound in helium films, *Physica B&C* **122**, 151 (1983).
9. P. W. Brouwer, W. A. Draisma, H. van Beelen, and R. Jochemsen, On the propagation of third sound in ^4He films, *Physica B* **215**, 135 (1995).
10. T. G. Wang and I. Rudnick, Anomalous attenuation of third sound, *J. Low Temp. Phys.* **9**, 425 (1972).
11. K. L. Telschow, R. K. Galkiewicz, and R. B. Hallock, Experiments on the attenuation of third sound in saturated superfluid helium films, *Phys. Rev. B* **14**, 4883 (1976).
12. K. C. Harvey and A. L. Fetter, Free surface of a rotating superfluid, *J. Low Temp. Phys.* **11**, 473 (1973).
13. F. M. Ellis and H. Luo, Low temperature exponential and liner free decay of 3rd sound resonances, *Physica B* **169**, 521 (1991).
14. F. M. Ellis and L. Li, Quantum swirling of superfluid helium films, *Phys. Rev. Lett.* **71**, 1577 (1993).
15. F. M. Ellis, L. Keeler, and C. Wilson, Pinned vortex density in He-4 films produced and detected by third sound resonances, *Physica B* **194-196**, 673 (1994).
19. K. W. Schwarz, Charge-carrier mobilities in liquid helium at the vapor pressure, *Phys. Rev. A* **6**, 873 (1972).
18. C. F. Barenghi, R. J. Donnelly, and W. F. Vinen, Friction on quantized vortices in helium II. A review, *J. Low Temp. Phys.* **52**, 189 (1983).
16. W. D. McCormick, D. L. Goodstein, and J. G. Dash, Adsorption and Specific-Heat Studies of Monolayer and Submonolayer Films of He^3 and He^4 , *Phys. Rev.* **168**, 249 (1968).
17. I. Rudnick, R. S. Kagiwida, J. C. Fraser, and E. Guyon, Third sound in adsorbed superfluid films, *Phys. Rev. Lett.* **20**, 430 (1968).
20. G. Baym, R. G. Barrera, and C. J. Pethick, Mobility of the electron bubble in superfluid helium, *Phys. Rev. Lett.* **22**, 20 (1969).
21. C. Zipfel and T. M. Sanders, *Proceedings of the Eleventh International Conference on Low Temperature Physics*, St. Andrews, Scotland, (1968).
22. R. Luusalo, A. Husmann, J. Kopu, and P. J. Hakonen, Pseudo-contact angle due to superfluid vortices in ^4He , *Europhys. Lett.* **50**, 222 (2000).
23. L. B. Lurio, T. A. Rabedeau, P. S. Pershan, I. F. Silvera, M. Deutsch, S. D. Kosowski, and B. M. Ocko, X-ray specular reflectivity study of the liquid-vapor density profile of ^4He , *Phys. Rev. B* **48**, 9644 (1993).
24. H. W. Jackson and P. V. Mason, Third-sound propagation in thick films of superfluid ^4He , *Phys. Rev. B* **42**, 7825 (1990).